American Mineralogist, Volume 71, pages 206–209, 1986

Lammerite, $Cu_3(AsO_4)_2$, a modulated close-packed structure

F. C. Hawthorne

Department of Earth Sciences, University of Manitoba
Winnipeg, Manitoba R3T 2N2, Canada

Abstract

The crystal structure of lammerite, $Cu_3(AsO_4)_2$, monoclinic, $a = 5.079(1)$, $b = 11.611(2)$, $c = 5.394(1)$ Å, $\beta = 111.72(2)°$, $V = 295.5(2)$ Å^3, $Z = 2$, space group $P2_1/a$, has been solved by direct methods and refined by a least-squares method of an R index of 3.1% using 822 observed ($I > 2.5\sigma$) reflections. Lammerite is a close-packed structure. There are α-PbO_2 type chains of octahedrally coordinated Cu running parallel to [100]. The chains are arranged in layers parallel to (001), and these layers are linked by arsenate tetrahedra and by additional Cu octahedra. The α-PbO_2 chains have been displaced from their ideal close-packed position by differential shear along [100], and the close-packed layers show a prominent modulation along [010]. Such a modulation is common in copper minerals containing edge-sharing octahedra; it would seem to be a cooperative effect of the local Jahn-Teller distortions around each Cu octahedron in the structure.

Introduction

Lammerite is a copper ortho-arsenate, $Cu_3(AsO_4)_2$, first characterized by Keller et al. (1981) from a hand specimen of corroded quartzose rock from Laurani, Bolivia. It was later reported from the Tsumeb copper deposit (Keller, 1981), where it is associated with chalcanthite, anhydrite, leightonite and various silicate minerals (Keller and Bartelke, 1982). As part of a general study of copper minerals (Hawthorne 1985a,b; Hawthorne and Groat, 1985a,b; Hawthorne and Eby, 1985), the structure of lammerite is examined here. Poulsen and Calvo (1968) reported the structure of a monoclinic form of $Cu_3(AsO_4)_2$, differing from that of lammerite. Keyite (Embrey et al., 1977) is a mineral from Tsumeb with the formula $(Cu, Zn, Cd)_3(AsO_4)_2$, different from lammerite or $Cu_3(AsO_4)_2$; it is not clear whether or not Cd is an essential component in keyite, this must await further structure work. Thus lammerite has at least one polymorph, adding further complexity to that already complex group, the $M_3(TO_4)_2$ minerals.

Experimental

The crystal used in this work is from the Tsumeb deposit, Namibia, and was obtained from the Department of Mineralogy and Geology, Royal Ontario Museum, collection number M38818. The crystal was mounted on a Nicolet R3m automated four-circle diffractometer, and the cell dimensions were refined from the setting angles of twenty-five automatically aligned intense reflections. The (monoclinically constrained) cell dimensions are listed in Table 1; they are statistically identical with those given by Keller et al. (1981).

Intensity data were collected according to the experimental procedure described by Hawthorne and Groat (1985a). A total of 869 reflections were measured out to a maximum 2θ of 60°. An empirical absorption correction was applied (ψ-scan method), approximating the crystal shape by a triaxial ellipsoid; R(symmetric) for the azimuthal data was reduced from 10.6% to 3.2%. Lorentz, polarization and background corrections were also done, and the data were reduced to structure factors; of the 869 unique reflections, 822 were classed as observed ($I > 2.5\sigma$).

Solution and refinement

Scattering curves for neutral atoms together with anomalous dispersion coefficients were taken from Cromer and Mann (1968) and Cromer and Liberman (1970). R indices are of the form given in Table 1 and are expressed as percentages.

The systematic absences $h0l$, $h = 2n + 1$; $0k0$, $k = 2n + 1$ uniquely define the space group as $P2_1/a$. The structure was solved by direct methods. The phase set with the highest combined figure of merit gave a solution that was compatible with the known stoichiometry. This refined rapidly to an R index of 4.6% for an isotropic thermal model. Conversion to anisotropic temperature factors for all atoms resulted in convergence at an R index of 3.1% for the 822 observed reflections. Final parameters are given in Table 2, observed and calculated structure factors and anisotropic temperature factor coefficients in Table 3[1] and interatomic distances and angles in Table 4. An empirical bond-valence calculation, using the parameters of Brown (1981) is given in Table 5.

[1] To receive a copy of Table 3, order Document AM-86-291 from the Business Office, Mineralogical Society of America, 1625 I Street, N.W., Suite 414, Washington, D.C. 20006. Please remit $5.00 in advance for the microfiche.

0003–004X/86/0102–0206$02.00

Table 1. Miscellaneous information: lammerite.

a	5.079(1)Å	Crystal size (mm)	0.18x0.20x0.35
b	11.611(2)	Rad/Mono	Mo/Gr
c	5.394(1)	Total unique |Fo|	869
β	111.72(2)°	No. of |Fo|>3 σ	822
V	295.5(2)Å^3	R(observed)	3.1%
Space Group	$P2_1/a$	R_w(observed)	3.5%

Unit cell contents: $2[Cu_3As_2O_8]$

$R = \Sigma(|Fo|-|Fo|)/\Sigma|Fo|$

$R_w = [\Sigma w(|Fo|-|Fc|)^2/\Sigma wFo^2]^{\frac{1}{2}}$, w = 1

Structural description

There is one unique arsenic position in lammerite; the As is coordinated by four O^{2-} anions, the resulting tetrahedron showing a typical range of bond-lengths and angles. The variation in As-O bond-lengths correlates well with the local bond-valence requirements of the anions (Table 5). There are two unique copper positions, each Cu being coordinated by six O^{2-} anions in distorted octahedral arrangements. Cu(1) is on special position 2*d*, a center of symmetry. It shows typical well-developed Jahn-Teller distortion, with four short meridional bonds (⟨Cu-O⟩ = 1.954 Å) and two long axial bonds (⟨Cu-O⟩ = 2.923 Å). Cu(2) is on the general position 4*e*, and hence has no symmetry constraints on its bond geometry. It also shows Jahn-Teller distortion, but it is not as strongly developed as for Cu(1), with four short meridonal bonds (⟨Cu-O⟩ = 1.972 Å) and two long axial bonds (⟨Cu-O⟩ = 2.532Å).

The structure of lammerite is illustrated in Figures 1 and 2. A prominent feature of the structure is the sheet of α-PbO_2 type staggered edge-sharing octahedral chains running parallel to [100] (Fig. 1); these consist of the Cu(2) octahedra that show the lesser amount of Jahn-Teller distortion of the two types of Cu octahedra in the structure. These chains are cross-linked in the two directions orthogonal to their lengths by the Cu(1) octahedra and As tetrahedra. It is difficult to see any further regularity in Figure 1 at first sight. However, Figure 2 provides the key to the rationalization of the structure. The staggered octahedral chains are seen end-on, and adjacent chains form layers orthogonal to [001]; between these layers are intercalated the highly distorted Cu(1) octahedra and the As tetrahedra. However, as is apparent in Figure 2, these layers are not planar but have a prominent modulation in the [010] direction, with an amplitude of ⅛ wave-length. An idealized version of two of these layers is shown in Figure 3. In a single close-packed double-layer of oxygen atoms, chains of edge-sharing octahedra are alternately

Table 2. Atomic parameters for lammerite.

	x	y	z	U^*_{equiv}
Cu(1)	0	1/2	1/2	1.25(3)
Cu(2)	0.2462(2)	0.8367(1)	0.8563(2)	1.48(3)
As	-0.1111(1)	0.8851(1)	0.2625(1)	0.96(2)
O(1)	0.1921(8)	0.9173(4)	0.2203(8)	1.3(1)
O(2)	-0.0946(9)	0.8157(4)	0.5390(8)	1.5(1)
O(3)	0.1717(9)	0.6871(4)	0.9904(8)	1.3(1)
O(4)	0.2893(9)	0.9902(4)	0.7332(8)	1.2(1)

$^*U_{equiv} = U_{equiv} \times 10^2$

Table 4. Selected interatomic distances (Å) and angles (°) for lammerite.

Cu(1)-O(1)a,b	1.974(4) x2	Cu(2)-O(1)f	2.282(5)
Cu(1)-O(2)c,d	2.923(5) x2	Cu(2)-O(2)	1.947(4)
Cu(1)-O(4)a,b	1.933(5) x2	Cu(2)-O(2)d	2.782(5)
⟨Cu(1)-O⟩	2.277	Cu(2)-O(3)	1.972(5)
		Cu(2)-O(3)d	2.028(4)
As-O(1)	1.680(5)	Cu(2)-O(4)	1.941(4)
As-O(2)	1.670(5)	⟨Cu(2)-O⟩	2.159
As-O(3)	1.695(4)		
As-O(4)b	1.713(4)		
⟨As-O⟩	1.690		
O(1)-O(2)	2.885(9)	O(1)-As-O(2)	118.9(2)
O(1)-O(3)	2.751(8)	O(1)-As-O(3)	109.2(2)
O(1)-O(4)b	2.766(8)	O(1)-As-O(4)b	109.2(2)
O(2)-O(3)	2.751(8)	O(2)-As-O(3)	109.7(2)
O(2)-O(4)b	2.673(8)	O(2)-As-O(4)b	104.4(2)
O(3)-O(4)b	2.695(8)	O(3)-As-O(4)b	104.5(2)
⟨O-O⟩As	2.754	⟨O-As-O⟩	109.3
O(1)a-O(2)c	3.587(10) x2	O(1)a-Cu(1)-O(2)c	92.1(1) x2
O(1)a-O(2)d	3.467(10) x2	O(1)a-Cu(1)-O(2)d	87.9(1) x2
O(1)a-O(4)a	2.758(9) x2	O(1)a-Cu(1)-O(4)a	89.8(2) x2
O(1)a-O(4)b	2.768(9) x2	O(1)a-Cu(1)-O(4)b	90.2(2) x2
O(2)c-O(4)a	4.173(10) x2	O(2)c-Cu(1)-O(4)a	117.0(2) x2
O(2)c-O(4)b	2.674(9) x2	O(2)c-Cu(1)-O(4)b	63.0(2) x2
⟨O-O⟩Cu(1)	3.238	⟨O-Cu(1)-O⟩	90.0
O(1)f-O(2)	3.614(10)	O(1)f-Cu(2)-O(2)	117.2(2)
O(1)f-O(3)	2.934(9)	O(1)f-Cu(2)-O(3)	86.9(2)
O(1)f-O(3)d	3.344(9)	O(1)f-Cu(2)-O(3)d	101.6(2)
O(1)f-O(4)	2.970(9)	O(1)f-Cu(2)-O(4)	89.0(2)
O(2)-O(2)d	2.963(9)	O(2)-Cu(2)-O(2)d	75.3(1)
O(2)-O(3)	2.747(9)	O(2)-Cu(2)-O(3)	89.0(2)
O(2)-O(4)	2.737(9)	O(2)-Cu(2)-O(4)	89.5(2)
O(2)d-O(3)	3.079(9)	O(2)d-Cu(2)-O(3)	78.7(2)
O(2)d-O(3)d	2.748(8)	O(2)d-Cu(2)-O(3)d	67.6(1)
O(2)d-O(4)	3.808(10)	O(2)d-Cu(2)-O(4)	106.1(2)
O(3)-O(3)d	2.930(9)	O(3)-Cu(2)-O(3)d	94.2(1)
O(3)d-O(4)	2.817(9)	O(3)d-Cu(2)-O(4)	90.4(2)
⟨O-O⟩Cu(2)	3.058	⟨O-Cu(2)-O⟩	90.5

a: 1/2-x, -1/2+y, 1-z; b: -1/2+x, 1/2-y+1, z; c: -1/2-x, -1/2+y, 1-z; d: 1/2+x, 1/2-y+1, z; e: -1/2+x, 1/2-y+1, z-1; f: x, y, z+1.

Table 5. Empirical bond-valence (v.u.) table for lammerite.

	Cu(1)	Cu(2)	As	Σ
O(1)	$0.435^{x2}_{\downarrow}$	0.182	1.263	1.880
O(2)	$0.041^{x2}_{\downarrow}$	0.472 0.055	1.309	1.877
O(3)		0.437 0.370	1.196	2.003
O(4)	$0.493^{x2}_{\downarrow}$	0.481	1.122	2.096
Σ	1.938	1.997	4.890	

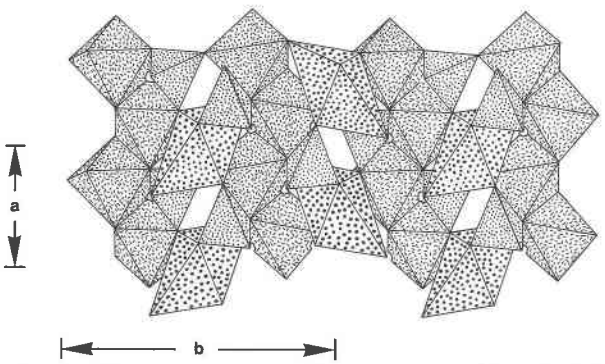

Fig. 1. The crystal structure of lammerite viewed down [001]; the Cu(1) octahedra are shaded in large dots, the Cu(2) octahedra are dashed and the As tetrahedra are dotted. Note the α-PbO_2 edge-sharing chains of octahedra parallel to **a**.

occupied (by Cu(2) atoms) and empty. A third layer of oxygen atoms overlies the first two to produce a cubic close-packed sequence. The As atoms occupy tetrahedral interstices in this second layer. The Cu(1) atoms occupy octahedral interstices in this second layer; however, they do not occupy completely regular octahedral sites (such as A, at which each octahedron shares 2 faces with As tetrahedra), but occupy axially compressed octahedra which share only 2 edges with adjacent As tetrahedra. In the real lammerite structure, adjacent edge-sharing chains are slightly displaced along [100]; as shown in Figure 4, this has the effect of shortening one pair of Cu(1)-O bonds and lengthening the other pair to produce an octahedron with a strong axial elongation. Thus lammerite is actually a cubic close-packed structure that has undergone slight differential shear together with a periodic layer modulation orthogonal to the shear direction.

The reason for the layer modulation can also be found in the spontaneous electronic relaxation of the structure. This is illustrated in Figure 5. If a planar layer of α-PbO_2 type octahedral chains is modulated such that the octahedral chains correspond to the maximum amplitude positions, one *trans* pair of bonds in each of the octahedra is elongated relative to the other four bonds. Thus modulation of the structure arises from the Jahn-Teller type distortion observed in the Cu(2) octahedra. Such modulations may be quite widespread in copper minerals; Haw-

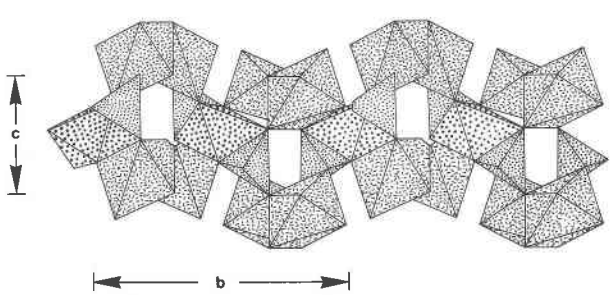

Fig. 2. The crystal structure of lammerite viewed down [100]; the shading is as in Fig. 1. Note the close-packed layers, moduled along **b**.

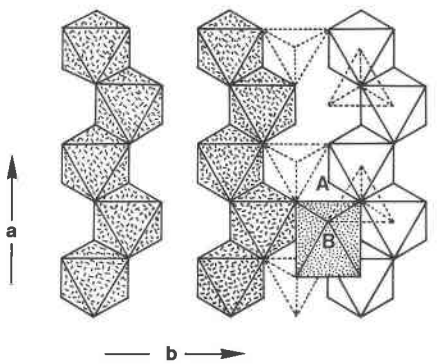

Fig. 3. The ideal close-packed lammerite arrangement. The chains of octahedra in the lower layer are alternately occupied (shaded) and vacant (not shaded), except for the rightmost occupied chain which is not shaded. The tetrahedra occupy the higher layer. The Cu of the higher layer does not occupy the regular octahedral site (such as A), but occupies the irregular octahedral site B (the large dotted octahedron).

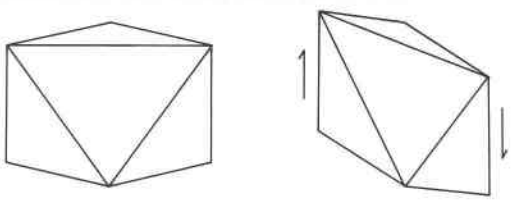

Fig. 4. This shows the effect of differential shear of the α-PbO_2 type chains, producing an axial elongation of the Cu(1) type octahedra. Note that this type of octahedron (site B in Fig. 3) is considerably shortened along the vertical direction; differential shear shortens one of the remaining pair of bonds and lengthens the other to produce elongation in a diagonal direction.

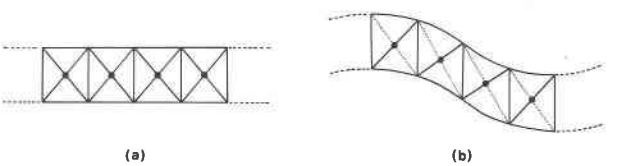

Fig. 5. The effect of layer modulation, producing an axial elongation of the Cu octahedra of the α-PbO_2 type chains. Of course, the modulation actually occurs because of the spontaneous distortion of the octahedra rather than vice versa.

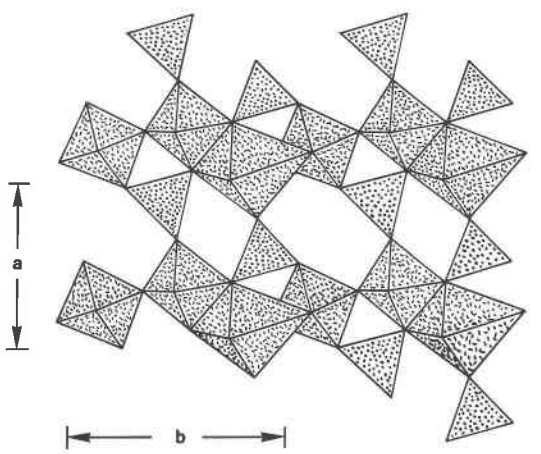

Fig. 6. The crystal structure of synthetic $Cu_3(AsO_4)_2$, projected down [001]; note the close-packed layers parallel to (110).

thorne and Eby (1985) showed that lingrenite is a modulated close-packed structure, and wroewolfeite (Hawthorne and Groat, 1985a), shattuckite and planchéite (Evans and Mrose, 1977) also show strong layer modulation.

A [001] projection of the synthetic $Cu_3(AsO_4)_2$ structure is shown in Figure 6. Two of the three unique Cu positions are [6]-coordinate, and the other is [5]-coordinate. The structure is close-packed with the rather corrugated anion layers running parallel to (110). The octahedral edge-sharing dimers prominent in Figure 5 link back along [001] to share corners with arsenate tetrahedra and the Cu(1) trigonal bipyramid; thus the layers have identical composition, and are characterized by a very open packing with few shared edges. This is apparent in the calculated densities of $Cu_3(AsO_4)_2$ and lammerite, which are 5.032 and 5.263 g/cm^3 respectively.

Acknowledgments

I am pleased to acknowledge the cooperation of Professors J. Mandarino and F. J. Wicks, curators at the Department of Mineralogy and Geology, Royal Ontario Museum, Hogtown. Financial support was provided by the National Sciences and Engineering Research Council of Canada, in the form of a fellowship, an operating grant, and a major equipment grant.

References

Brown, I. D. (1981) The bond-valence method: an empirical approach to chemical structure and bonding. *In* M. O'Keefe and A. Navrotsky (Eds.), Structure and Bonding in Crystals, Vol. II, p. 1–30. Academic Press, New York.

Cromer, D. T. and Liberman, David (1970) Relativistic calculation of anomalous scattering factors for X-rays. Journal of Chemical Physics, 53, 1891–1898.

Cromer, D. T. and Mann, J. B. (1968) X-ray scattering factors computed from numerical Hartree-Fock wave functions. Acta Crystallographica, A24, 321–324.

Embrey, P. G., Fejer, E. E. and Clark, A. M. (1977) Keyite: A new mineral from Tsumeb. Mineralogical Record, 8, 87–90.

Evans, H. T., Jr. and Mrose, M. E. (1977) The crystal chemistry of the hydrous copper silicates, shattuckite and planchéite. American Mineralogist, 62, 491–502.

Groat, L. A. and Hawthorne, F. C. (1985) Refinement of the crystal structure of papagoite. Tschermaks Mineralogische und Petrographische Mitteilungen, in press.

Hawthorne, F. C. (1985a) Towards a structural classification of minerals. The $^{VI}M^{IV}T_2\phi$ minerals. American Mineralogist, 70, 455–473.

Hawthorne, F. C. (1985b) Refinement of the crystal structure of botallackite. Mineralogical Magazine, 49, 85–89.

Hawthorne, F. C. and Eby, R. (1985) Refinement of the crystal structure of lindgrenite. Neues Jahrbuch für Mineralogie, 1985, 234–240.

Hawthorne, F. C. and Groat, L. A. (1985) The crystal structure of wroewolfeite, a mineral with $[Cu_4(OH)_6(SO_4)(H_2O)]$ sheets. American Mineralogist, 70, 1050–1055.

Keller, P. (1981) Lammerit, $Cu_3(AsO_4)_2$, und seine Paragenses in Tsumeb. Der Aufschluss, 32, 437–441.

Keller, P. and Bartelke, W. (1982) Tsumeb! New minerals and their associations. Mineralogical Record, 13, 137–147.

Poulsen, S. J. and Calvo, C. (1968) Crystal structure of $Cu_3(AsO_4)_2$. Canadian Journal of Chemistry, 46, 917–927.

Manuscript received, April 23, 1985;
accepted for publication, September 4, 1985.